A Three-dimensional Ferric Molybdenum(V) Phosphate Network with Tunnels: Synthesis, Structure, Magnetic and Electrochemical Properties

Kai Yu[a,b], Bai-bin Zhou[a,b], Yang Yu[c], and Zhan-hua Su[b]

[a] School of Chemical Engineering, Harbin Institute of Technology, Harbin 150001, P. R. China
[b] Key Laboratory of Synthesis of Functional Materials and Green Catalysis, Colleges of Heilongjiang Province, Harbin Normal University, Harbin 150080, P. R. China
[c] Water Quality Center, Harbin Water Supply Drainage Group Co., Ltd., Harbin 150080, P. R. China

Reprint requests to Dr. Baibin Zhou. E-mail: zhou_bai_bin@163.com

Z. Naturforsch. **2011**, *66b,* 49 – 54; received August 23, 2010

A reduced ferric molybdophosphate, $(H_2en)_3(Hen)[Fe^{III}_3Mo^{V}_{12}O_{24}(OH)_8(HPO_4)_4(PO_4)_4]\cdot 3H_2O$ (**1**) has been hydrothermally synthesized and characterized. In compound **1**, a sandwich-shaped cluster $[Fe(Mo_6P_4)_2]$ is connected to eight peripheral $\{FeO_5(OH)\}$ octahedra through its eight $\{PO_4\}$ tetrahedra to form a three-dimensional framework with channels which are filled by water and protonated ethylenediamine molecules. The compound exhibits a 4,8-connected 3-D network with a $(4^{12}6^{12}8^4)(4^6)_2$ topology. The DC susceptibility measurement has shown an antiferromagnetic character of the exchange interactions. Additionally, the electrochemical properties of **1**-CPE were studied in detail.

Key words: Hydrothermal Synthesis, Ferric Molybdophosphate, Three-dimensional Framework, Topology, Magnetic Character

Introduction

Current interest in polyoxometalates (POMs) is rapidly expanding owing to their intriguing structures and topological features as well as their potential applications in catalysis, molecular adsorption, medicine, electro-conductivity, magnetism, and photochemistry [1]. The construction of POMs with differently extended dimensionality and with controllably tailored properties has become a very important subject. One important strategy for the synthesis of POMs is to utilize hydrothermal synthesis methods to find some suitable bridging units and then to link POM building units up into extended solid frameworks. More recently, a wide variety of molybdenum phosphates with transition metals has been synthesized and characterized [2]. However, due to the limits of coordination numbers of bridging units and the steric hindrance issues of most POMs, it is very difficult to construct highly connected coordination frameworks.

Notably, in the large POM family, the reduced molybdophosphates containing Mo–Mo bonds are an important subclass and have wide application in catalysis owing to their microporous character and also to their redox properties. The $P_4Mo_6X_{31}$ { X = O, OH } POMs with various degrees of protonation have been regarded as suitable anionic templates to build up 3-D and highly connected structures. At these very stable structural units, the highly active surface oxygen atoms of $[P_4Mo_6]$ can be easily engaged in bonding with alkali metals and many transition metals to form 1-D chains [3] or 2-D polymers [4] and 3-D networks [5]. However, in comparision with the variety of other transition metal hybrid compounds, the 3-D $[P_4Mo_6]$ POMs containing iron have remained relatively undeveloped, and only a few examples have been reported so far [6]. Therefore, it remains a great challenge to design and synthesize new highly connected organic-inorganic hybrid POMs with a new structure topology. So we have turned our attention to the construction of binodal and highly connected $[P_4Mo_6]$-based hybrids with iron cations.

As it is difficult to predict the exact structures and conformations of the final products, we carried out a series of hydrothermal reactions by changing the reaction conditions, such as temperature, molar ratios, counterions and so on. Fortunately, we have thereby synthesized and structurally characterized the target, 3-D reduced ferric molybdophosphate with $(4^{12}6^{12}8^4)(4^6)_2$ topology, $[(H_2en)_3(Hen)][Fe^{III}{}_3$-

$Mo_{12}{}^{V}O_{24}(OH)_8(HPO_4)_4(PO_4)_4]\cdot 3H_2O$ (**1**). To our knowledge, a three-dimensional, binodal and eight-connected network structure which is formed from molybdenum(V) phosphate units interconnected only with iron cations has not been reported up to now. The magnetic and electrochemical properties of compound **1** were also investigated.

Results and Discussion

*Crystal structure of **1***

The single-crystal X-ray analysis revealed that the structure of compound **1** consists of $[P_4Mo_6]$ units, iron cations, mono- and di-protonated en molecules and lattice water molecules. As usually observed, each $[P_4Mo_6]$ unit is made up of six $\{MoO_6\}$ octahedra and four $\{PO_4\}$ tetrahedra. The six $\{MoO_6\}$ octahedra are coplanar and constitute a hexanuclear molybdenum ring with alternating Mo–Mo (2.591 ~ 2.592 Å) bonds and non-bonding Mo–Mo contacts (3.518 ~ 3.527 Å). Four $\{PO_4\}$ tetrahedra are linked to the ring by sharing corners with three $\{PO_4\}$ groups around the periphery of the ring and the other group located in its center (Fig. 1a). The P–O bond lengths are in the range from 1.487(3) to 1.583(3) Å, and the O–P–O bond angles vary from 104.45(17)° to 115.38(19)°. The Mo–O distances are in the range 1.676(3) ~ 2.299(3) Å. There are two types of Fe^{3+} cations, which exhibit two kinds of coordination environments in compound **1**. One octahedrally coordinated Fe^{3+} cation (Fe(1)) is linked to two $\{Mo_6\}$ rings *via* three μ-O atoms (O(3), O(4), O(7)) with Fe–O bond lengths of 2.164(3), 2.213(3), and 2.202(3) Å, respectively (Fig. 1b). The other Fe^{3+} cation is octahedrally coordinated by one -OH group and five oxygen atoms shared with five $\{PO_4\}$ tetrahedra from four neighboring $[P_4Mo_6]$ units. Two of the five $\{PO_4\}$ tetrahedra are from the same $[Fe(1)(Mo_6P_4)_2]$ cluster, and the other three are from different $[Fe(1)(Mo_6P_4)_2]$ clusters. Interestingly, each $[Fe(1)(Mo_6P_4)_2]$ unit contacts eight different, but crystallographically identical, Fe(2) atoms through its eight $\{PO_4\}$ tetrahedra in corner-sharing mode (Fig. 2). Compound **1** is a 4,8-connected three-dimensional framework with $(4^{12}6^{12}8^4)(4^6)_2$ topology (Fig. 3). In this simplification, the 8-connected nodes are $[Fe(1)(Mo_6P_4)_2]$ clusters, and the 4-connected ones are Fe(2) centers. The distances between Fe(1) and

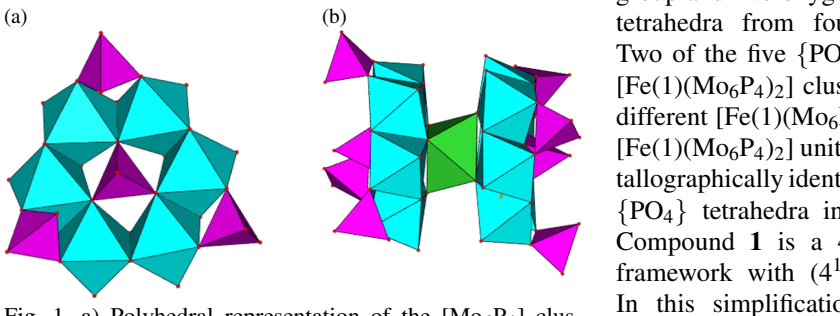

Fig. 1. a) Polyhedral representation of the $[Mo_6P_4]$ cluster; b) polyhedral representation of the centrosymmetric $[Fe(1)(Mo_6P_4)_2]$ unit.

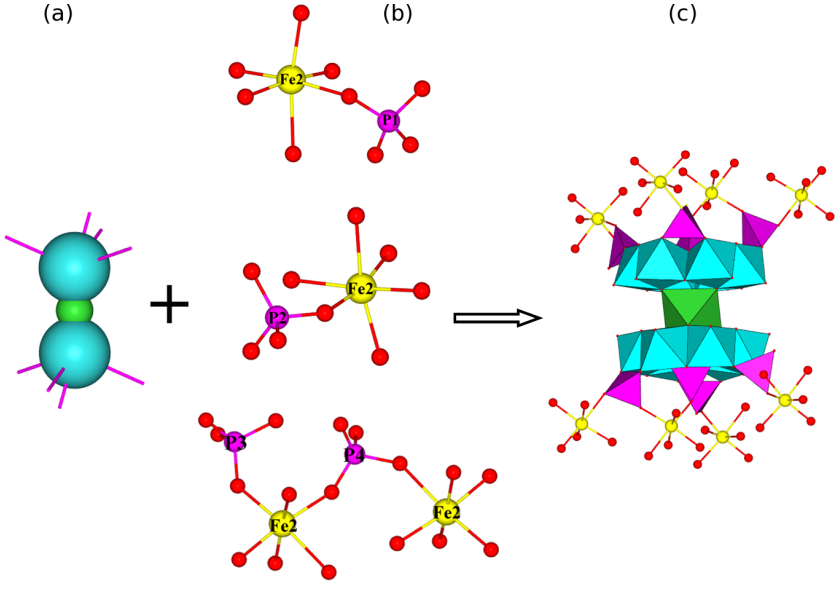

Fig. 2. a) Representation of the coordination of the $Fe[Mo_6P_4]_2$ units; b) representation of the coordination modes of the $Fe(2)^{3+}$ cation with phosphate; c) representation of the highly connected sandwich-type POMs due to the aggregation of modes a) and b).

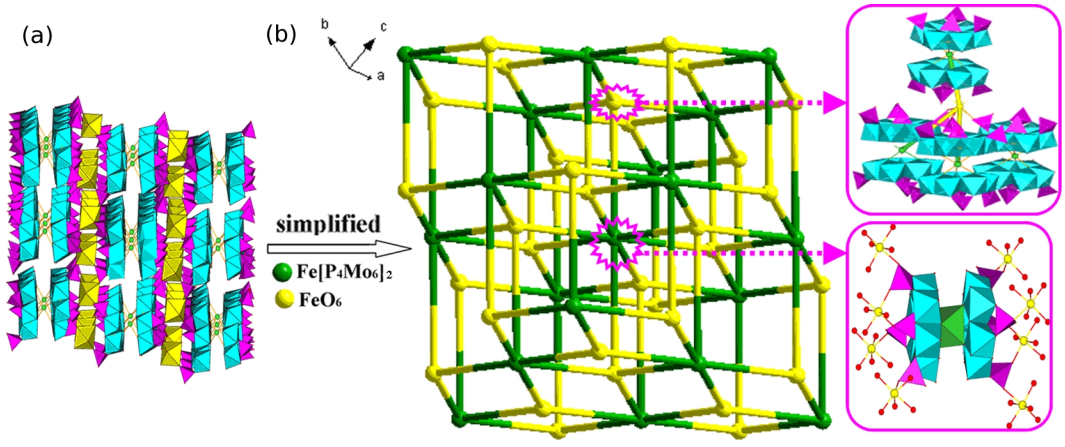

Fig. 3 (color online). a) Polyhedral representation of the 3D structure of compound **1**; b) view of the topology of compound **1** (the green nodes symbolize the [Fe(1)(Mo_6P_4)$_2$] clusters, and the yellow nodes symbolize {Fe(2)O_6} octahedra).

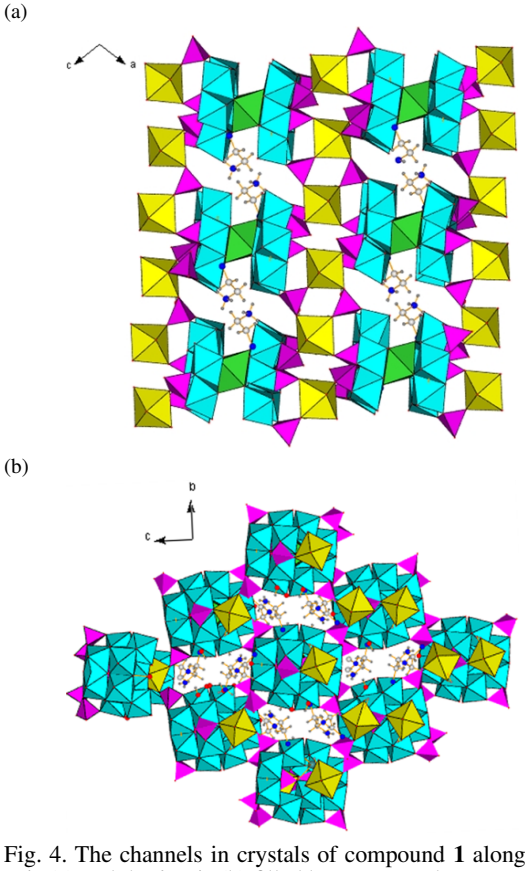

Fig. 4. The channels in crystals of compound **1** along the *a* axis (a) and the *b* axis (b) filled by protonated en.

Fe(2) are 7.062, 9.394, 9.432 and 9.827 Å. Moreover, the [Fe(Mo_6P_4)$_2$] building blocks are linked by [FeO_5(OH)] octahedra in a corner-sharing mode to form a 3-D framework with channels (Fig. 4). This organization leads to the petalous shape of channels along the *b* axis, which are surrounded by two [Fe(1)(Mo_6P_4)$_2$] units and two Fe(2) cations with a size of *ca.* 12.131 × 14.940 Å^2 based on the Fe(1)–Fe(1) and Fe(2)–Fe(2) distances (Fig. 4a). This connectivity generates the parallelogramm-like shape of the channels along the *a* axis, which are surrounded by four [Fe(1)(Mo_6P_4)$_2$] units, with a size of *ca.* 8.313 ×

Table 1. Crystal data and structure refinement parameters for **1**.

Formula	$C_8H_{57}Fe_3Mo_{12}N_8O_{67}P_8$
M_r	2890.02
Crystal. size, mm^3	0.20 × 0.16 × 0.12
Crystal system	monoclinic
Space group	$P2_1/n$
a, Å	16.2045(13)
b, Å	11.8680(9)
c, Å	17.9591(14)
β, deg	103.6440(10)
V, Å^3	3356.3(5)
Z	2
D_{calcd}, g cm^{-3}	2.85
μ (MoK_α), cm^{-1}	3.1
F(000), e	5733
hkl range	±21, ±15, ±23
θ range, deg	2.59 – 28.35
Reflections collected / unique / R_{int}	33217 / 8320 / 0.0218
Data / restraints / parameters	8320 / 1530 / 485
$R1$ / $wR2$[a] [$I \geq 2\,\sigma(I)$]	0.0312/0.0916
$R1(F)$ / $wR2$[a] (all refl.)	0.0342 / 0.0940
GoF[b] (F^2)	1.052
$\Delta\rho_{fin}$ (max / min), e Å^{-3}	3.40 / −2.31

[a] $R1 = \Sigma||F_o| - |F_c||\Sigma|F_o|$, $wR2 = [\Sigma w(F_o^2 - F_c^2)^2/\Sigma w(F_o^2)^2]^{1/2}$, $w = [\sigma^2(F_o^2)+(0.484P)^2+24.2999P]^{-1}$, where $P = (\mathrm{Max}(F_o^2, 0)+2F_c^2)/3$; [b] GoF = $[\Sigma w(F_o^2 - F_c^2)^2/(n_{obs} - n_{param})]^{1/2}$.

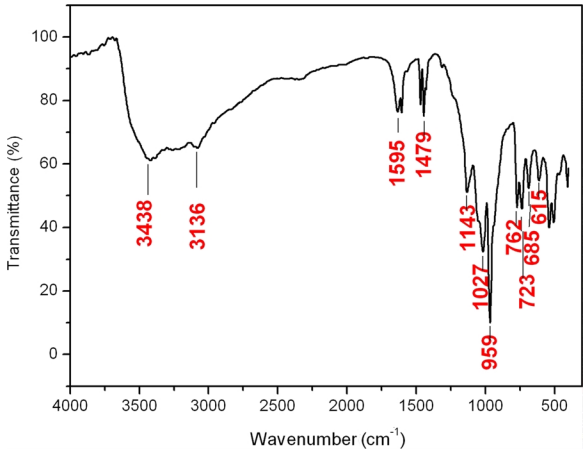

Fig. 5. IR spectrum of compound **1**.

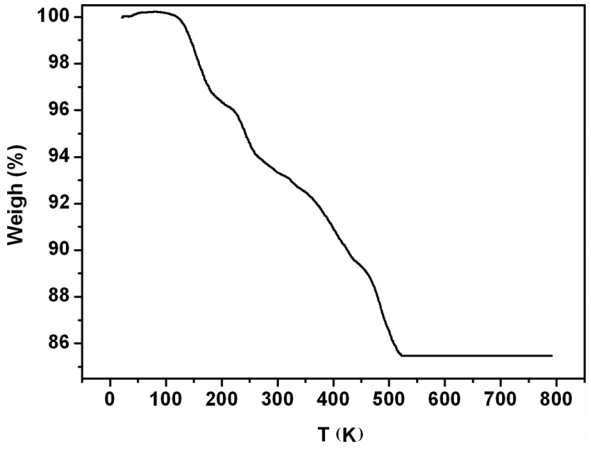

Fig. 6. TG curve of compound **1**.

3.227 Å^2 based on O(15)–O(15) and O(17)–O(17) distances (Fig. 4b). Free protonated ethylenediamine (H_2en) units and water molecules are located in these tunnels (Fig. 4).

To date, a three-dimensional and eight-connected open network structure which is constructed from molybdenum(V) phosphate, interconnected only with iron cations, has not been reported.

The crystallographic and structure determination data of compound **1** are summarized in Table 1. On the basis of bond valence sum (BVS) calculations [8], all Mo and Fe centers are in the oxidation states of +5 and +3, respectively. The oxidation states of the Mo and Fe atoms are consistent with the formula of compound **1**.

IR spectrum

In the IR spectrum of compound **1** (Fig. 5), the strong bands at 959 cm^{-1} are due to the ν(Mo=O) vibrations. The strong bands at 1027 and 1143 cm^{-1} are attributed to ν(P-O). Features at 762, 723, 685, and 615 cm^{-1} are associated with ν(Mo-O-Mo). The bands at 1479, 1595 and 3438 cm^{-1} can be regarded as the vibrations of the H_2 en cations, while the characteristic band at 3136 cm^{-1} is ascribed to water molecules.

Thermal analysis

The X-ray diffraction analysis has confirmed that compound **1** contains a certain amount of coordinated water and clathrate water molecules, making a TG analysis indispensable. The thermogravimetric analysis of compound **1** carried out from 25 to 800 °C (Fig. 6) shows three major weight losses. The first and second weight losses of 6.8 % in the temperature range of 120 – 280 °C correspond to the release of all crystal lattice and coordinated water molecules in accordance with the calculated value of 6.85 % (∼11 H_2O). The third weight loss of 8.3 % in the temperature range of 280 ∼ 500 °C is attributed to the loss of all en molecules. The value is close to the calculated value of 8.30 % (∼ 4 H_2en). The overall weight loss of 15.1 % is in accordance with the calculated value of 15.15 %.

*Voltammetric behavior of **1**-CPE*

To determine the redox properties of compound **1**, a **1**-bulk-modified carbon paste electrode (**1**-CPE) was fabricated as the working electrode due to its insolubil-

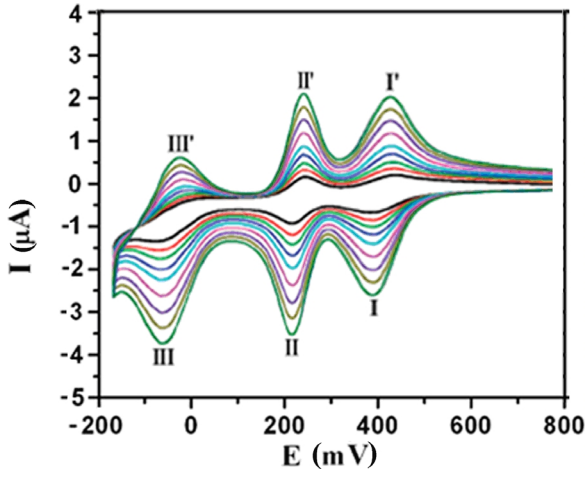

Fig. 7. Cyclic voltammograms of the **1**-CPE in 1 M H_2SO_4 solution at different scan rates (from inner to outer: 20, 40, 60, 100, 140, 180, 220, 260, 300 mV s^{-1}).

ity in water and common organic solvents. The cyclic voltammetric behavior for 1-CPE in 1 M H_2SO_4 aqueous solution was investigated at different scan rates was investigated. Three reversible redox couples were observed in the potential range from −200 to 800 mV shown in Fig. 7. The half-wave potentials $E_{1/2} = (E_{pa} + E_{pc})/2$ were −46 (III–III′), 226 (II–II′) and 398 mV (I–I′) (scan rate: 100 mV s^{-1}). Every redox peak corresponds to a one-electron redox process of Mo [9]. The cathodic peak potentials shift to the negative direction, and the corresponding anodic peak potentials shift to the positive direction with increasing scan rates. The peak-to-peak separations between the corresponding anodic and cathodic peaks increase, but the average peak potentials do not change on the whole.

Magnetic properties

The DC magnetic susceptibility (χ_m) data were measured in the temperature range of 2 – 300 K in a 1000 Oe magnetic field and are plotted as $\chi_m T$ *vs.* T in Fig. 8 for **1**. The product $\chi_m T$ of 13.25 cm^3 K mol^{-1} at 300 K decreases continuously to 10.08 $cm^3 \cdot K \cdot mol^{-1}$ at 2 K. The $\chi_m T$ value at r. t. is a little lower than the expected value ($\chi_m T$ = 13.13 cm^3 K mol^{-1}) for 3 uncoupled Fe^{III} ions (S = 5/2, C = 4.375 cm^3 K mol^{-1}) taking into account the g value of 2.0. This result suggests that all delocalized electrons in the polyoxoanion cluster might be totally antiferromagnetically coupled. The $1/\chi_m$ *vs.* T curve is consistent with the Curie-Weiss law between 2 and 300 K with C = 13.21 cm^3 K mol^{-1} and $\theta = -0.74$ K. The negative Weiss constant (θ) suggests the presence of mainly antiferromagnetic interactions between the Fe^{III} cations in compound **1**.

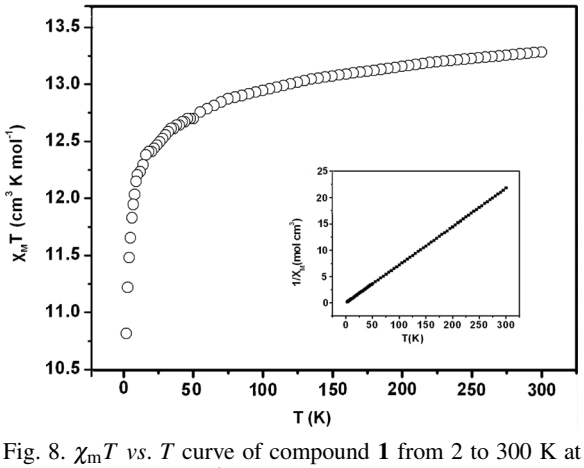

Fig. 8. $\chi_m T$ *vs.* T curve of compound **1** from 2 to 300 K at H = 1 kOe (insert: χ_m^{-1} *vs.* T curve of compound **1**.)

Conclusion

In summary, a new ferric molybdophosphate based on $[P_4Mo_6]$ units has been synthesized and characterized. In the compound **1**, a sandwich-shaped cluster $[Fe(Mo_6P_4)_2]$ is connected to its peripheral eight $\{FeO_5(OH)\}$ octahedra through its eight $\{PO_4\}$ tetrahedra into a three-dimensional framework with channels which are filled with mono- and diprotonated ethylenediamine and water molecules. It represents the first 4,8-connected 3-D organic-inorganic hybrid POM in the $\{P_4Mo_6/Fe\}$ series. The isolation of compound **1** shows that the $[P_4Mo_6]$ cluster is a good inorganic ligand to build 3-D and highly connected structures.

Experimental Section

General procedures

All chemicals were commercially purchased and used without further purification. Elemental analyses (C, H and N) were performed on a Perkin–Elmer 2400 CHN elemental analyzer. The contents of Fe, Mo, and P were determined by a Leaman inductively coupled plasma (ICP) spectrometer. FTIR spectra were recorded in the range of 4000 – 400 cm^{-1} on an Alpha Centaur FTIR spectrophotometer using KBr pellets. The TG analyses were performed on a Perkin-Elmer TGA7 instrument under flowing N_2 with a heating rate of 10 K min^{-1}. The magnetic susceptibility data were measured with a Quantum Design SQUID magnetometer MPMS-XL in the temperature range of 2 – 300 K at 1000 Oe.

*Preparation of $(H_2en)_3(Hen)[Fe^{III}{}_3Mo_{12}{}^{V}O_{24}(OH)_8(HPO_4)_4(PO_4)_4] \cdot 3H_2O$ (**1**)*

Compound **1** was prepared by the hydrothermal method: $Na_2MoO_4 \cdot 2H_2O$ (1.452 g, 6.00 mmol), $FeSO_4 \cdot 7H_2O$ (0.512 g, 2.3 mmol), ethylenediamine (0.6 mL, 8.98 mmol), H_3PO_4 (2 mL, 30 mmol), and 2, 6-pyridinedicarboxylic acid (0.35 g, 2.09 mmol) were dissolved in 36 mL of water. The mixture was stirred for 0.5 h at r. t. and then heated in a 50 mL Teflon-lined stainless steel autoclave for 6 d at 180 °C. After the autoclave was cooled to r. t., deep-red block-shaped crystals were harvested, washed with distilled water and dried at r. t. (yield 45.6 % based on Mo). Elemental analyses (%): calcd. C 3.30, H 1.99, Fe 5.75, Mo 39.85, N 3.84, P 8.62; found C 3.32, H 1.97, Fe 5.80, Mo 39.83, N 3.87, P 8.57.

*Preparation of **1**-CPE*

The **1**-CPE was prepared as follows: graphite powder (0.3 g) and compound **1** (0.03 g) were mixed and ground together in an agate mortar and pestle to achieve a uniform mixture, and Nujol (0.2 mL) was then added with stirring.

The resulting paste was packed in a glass tube (3 mm diameter), and a copper rod was inserted through one end of the tube to make electrical contact.

X-Ray crystallography

A deep-red block-shaped single crystal with dimensions of 0.20 × 0.16 × 0.12 mm^3 was mounted on a glass fiber. Single-crystal X-ray data of compound **1** were collected on a Bruker SMART CCD diffractometer equipped with graphite-monochromatized MoK_α radiation (λ = 0.71073 Å). A semiempirical absorption correction was applied using the program SADABS. The structure was solved by Direct Methods and refined by full-matrix least-squares methods on F^2 using the SHELXTL-97 software package [7]. All non-hydrogen atoms were refined anisotropically. Hydrogen atoms on carbon and nitrogen atoms were included at calculated positions and refined with a riding model. The crystallographic and structure determination data of compound **1** are summarized in Table 1.

CCDC 768658 contains the supplementary crystallographic data for this paper. These data can be obtained free of charge from The Cambridge Crystallographic Data Centre *via* www.ccdc.cam.ac.uk/data_request/cif.

Acknowledgement

This work was supported by the National Natural Science Foundation of China (Grant Nos. 20671026 and 20971032), the Study Technological Innovation Project Special Foundation of Harbin (2009RFXXG202), and the Science and Technology Project of Education Office of Heilongjiang Province (11551122), the Technological Innovation Team Building Program of the College of Heilongjiang Province (2009td04), and the Innovation Team Research Program of Harbin Normal University (KJTD200902).

[1] a) P. Gouzerh, A. Proust, *Chem. Rev.* **1998**, *98*, 77; b) P. Gouzerh, R. Villanneau, R. Delmont, A. Proust, *Chem. Eur. J*. **2000**, *6*, 1184; c) C. L. Hill, (Ed.), *Chem. Rev.* **1998**, *98*, 1 – 390, (special issue on polyoxometalates); d) M. T. Pope, A. Müller, (Eds.), *Polyoxometalate Chemistry*: *From Topology Via Self-Assembly to Applications*, Kluwer, Dordrecht, **2001**; e) T. Yamase, M. T. Pope, (Eds.), *Polyoxometalate Chemistry for Nano-Composite Design*, Kluwer, Dordrecht, **2002**; f) D. L. Long, E. Burkholder, L. Cronin, *Chem. Soc. Rev*. **2007**, *36*, 105.

[2] a) D. L. Long, E. Burkholder, L. Cronin, *Chem. Soc. Rev*. **2007**, *36*, 105; b) W. J. Chang, Y. C. Jing, S. L. Wang, K. H. Lii, *Inorg. Chem.* **2006**, *45*, 6586.

[3] a) Y. S. Zhou, L. J. Zhang, X. Z. You, S. Natarajan, *Inorg. Chem. Commun.* **2001**, *4*, 699; b) Y. S. Zhou, L. J. Zhou, X. Z. You, S. Natarajan, *Int. J. Inorg. Mat.* **2001**, *3*, 373; c) F. N. Shi, F. A. Paz, P. I. Girginova, H. I. S. Nogueira, J. Rocha, V. S. Amaral, A. Makal, J. Klinowski, T. Trindade, *J. Solid State Chem.* **2006**, *179*, 1497; d) H. X. Guo, S. X. Liu, *J. Mol. Struct*. **2005**, *751*, 156; e) S. T. Wang, E. B. Wang, Y. Hou, Y. G. Li, L. Wang, M. Yuan, C. W. Hu, *Transition Met Chem.* **2003**, *28*, 618; f) J. Zhang, Y. S. Zhou, X. Q. Li, Y. H. Li, *J. Clust. Sci*. **2007**, *18*, 921.

[4] a) Y. Ma, Y. G. Li, E. B. Wang, Y. Lu, X. L. Wang, X. X. Xu, *J. Solid State Chem*. **2006**, *179*, 2367; b) X. Z. Liu, B. Z. Lin, L. W. He, X. F. Huang, Y. L. Chen, *J. Mol. Struct*. **2008**, *877*, 72; c) X. Q. Chen, S. Lin, L. J. Chen, X. H. Chen, C. L. Liu, J. B. Chen, L. Y. Yang, *Inorg. Chem. Commun*. **2007**, *10*, 1285.

[5] a) X. He, P. Zhang, T. Y. Song, Z. C. Mu, J. H. Yu, Y. Wang, J. N. Xu, *Polyhedron* **2004**, *23*, 2153; b) H. X. Guo, S. X. Liu, *J. Mol. Struct*. **2005**, *741*, 229; c) L. Y. Duan, F. C. Liu, X. L. Wang, E. B. Wang, C. Qin, Y. G. Li, X. L. Wang, C. W. Hu, *J. Mol. Struct.* **2004**, *705*, 15; d) A. Leclaire, M. M. Borel, A. Guesdon, R. E. Marsh, *J. Solid State Chem*. **2001**, *159*, 7; e) M. Yuan, E. B. Wang, Y. Lu, Y. G. Li, C. W. Hu, N. H. Hu, H. Q. Jia, *J. Solid State Chem*. **2003**, *170*, 192.

[6] a) L. A. Meyer, R. C. Haushalter, *Inorg. Chem*. **1993**, *32*, 1579; b) L. X. Y. Q. Sun, E. B. Wang, E. H. Shen, Z. R. Liu, C. W. Hu, Y. Xing, Y. H. Lin, H. Q. Jia, *Inorg. Chem. Commun*. **1998**, *1*, 382.

[7] G. M. Sheldrick, SHELXS/L-97, Programs for Crystal Structure Determination, University of Göttingen, Göttingen (Germany), **1997**; See also: G. M. Sheldrick, *Acta Crystallogr*. **2008**, *A64*, 112.

[8] I. D. Brown, D. Altermatt, *Acta Crystallogr*. **1985**, *B41*, 244.

[9] J. Chen, J. Q. Sha, J. Peng, Z. Y. Shi, B. X. Dong, A. X. Tian, *J. Mol. Struct*. **2007**, *846*, 128.